Journal of Luminescence 194 (2018) 485–493

Contents lists available at ScienceDirect

Journal of Luminescence

journal homepage: www.elsevier.com/locate/jlumin

Tuning the photoluminescence of Eu^{2+} and Eu^{3+} co-doped $SrSO_4$ through post annealing technique

Bao-gai Zhai, Daqing Liu, Yong He, Long Yang, Yuan Ming Huang*

School of Mathematics and Physics, Changzhou University, Jiangsu 213164, China

A R T I C L E I N F O

Keywords:
Photoluminescence
Thermal annealing
Oxygen vacancy
Band structure
Density functional calculations

A B S T R A C T

Eu^{2+} and Eu^{3+} co-doped $SrSO_4$ microcrystals were synthesized by employing Eu^{3+} as the sole doping source in the precipitation synthesis. As the annealing temperature increases from 200 to 1000 °C, it is found that the broad photoluminescence (PL) band of Eu^{2+} peaking at 378 nm is dramatically enhanced in intensity as the cost of the narrowband emissions of Eu^{3+} at 584, 591 and 612 nm, respectively. Moreover, Two broad PL bands, one of which is centered at 500 nm while the other is centered at 625 nm, are recorded upon post annealing. On the basis of density functional calculations, post annealing introduced oxygen vacancy is proposed to play critical roles in tuning the PL of Eu^{2+} and Eu^{3+} co-doped $SrSO_4$. On one hand, the oxygen vacancy is responsible for the enhanced emission of Eu^{2+} at 378 nm by reducing Eu^{3+} to Eu^{2+}. On the other hand, the oxygen vacancy acts as electron trap and luminescence center in $SrSO_4$ with the result of the broad PL band centered at 500 nm. Our results have demonstrated that the PL of Eu^{2+} and Eu^{3+} co-doped $SrSO_4$ microcrystals can be tuned by simply varying the post annealing temperature.

1. Introduction

Rare-earth activated $SrSO_4$ has found wide applications in radiation dosimetry with the merit of high sensitivity to low-level radioactivity [1–6]. The rare earth ions in $SrSO_4$, such as Tb^{3+} [2,6], Eu^{2+} [3–5] and Dy^{3+} [6], work as luminescence centers to give off efficient emissions under the X-ray and gamma ray irradiations. Apart from working as thermoluminescent materials, $SrSO_4$, which is a typical insulator with a wide bandgap of about 7.6 eV [7], can also be utilized as the host of rare-earth dopants for the development of efficient phosphors under ultraviolet (UV) excitation. Indeed, several groups reported the photoluminescence (PL) of rare-earth doped $SrSO_4$ upon UV excitation. For example, Di et al. [8] reported the violet-blue PL of Eu^{2+} doped $SrSO_4$ under the excitation of 260 nm, Gong et al. [9] separately recorded the PL of Eu^{2+} and Eu^{3+} doped $SrSO_4$ under the excitation of 246 nm, Sun et al. [10] explored the orange PL of Sm^{3+} doped $SrSO_4$ under the excitation of 401 nm, and Yamashita et al. [11] observed the green PL of Tb^{3+} doped $SrSO_4$ under the excitation of 352 nm. These results have unveiled the potential of rare-earth doped $SrSO_4$ as efficient phosphors for LED and other information display devices. However, there are a number of drawbacks found in the existing researches on rare-earth doped $SrSO_4$. The first drawback is that tunable PL is not realized for rare-earth doped $SrSO_4$. For instance, Gong et al. [9] recorded the characteristic emissions of both Eu^{3+} and Eu^{2+} in the gamma-ray irradiated $SrSO_4$ nanocrystals, but they left the task of tuning the emissions of Eu-doped $SrSO_4$ unattended. The second drawback is that the mechanism leading to the generation of vacancies in $SrSO_4$ has not been investigated. Although $SrSO_4$ has been employed as the host for a variety of rare-earth dopants, there is lack of information about the defect properties in these materials, especially those doped with Eu^{3+} [9–11]. It is known that vacancies and other defects in host materials play a vital role in the PL properties. Due to thermal fluctuation, for example, oxygen vacancy (V_O) occur naturally in all crystalline materials at any given temperature up to the melting point of the material. Moreover, strong perturbation of space charge neutrality occurs and self compensation induced vacancies can be produced when extrinsic defect Eu^{3+} ions are present in $SrSO_4$ since an Eu^{3+} ion is not an isovalent impurity to the metal cation Sr^{2+}. Both the intrinsic defects such as V_O and the extrinsic defects such as Eu^{3+} allow new electronic states to exist within the band gap, electrons and/or holes can be trapped by them and then recombine with each other resulting in either radiative or non-radiative luminescence of photons. To the best of our knowledge, the V_O introduced emissions in $SrSO_4$ have not been reported.

To meet the increasing demand of phosphors for LED industry, it is significant to develop color tunable $SrSO_4$ phosphors. The general strategy for tuning the PL of rare-earth doped material is to dope the host with two species of rare-earth ions, and tunable emissions can be achieved by varying the concentrations of the dopants in the host. This

---

* Corresponding author.
E-mail address: dongshanisland@126.com (Y.M. Huang).

http://dx.doi.org/10.1016/j.jlumin.2017.10.078
Received 12 April 2017; Received in revised form 17 September 2017; Accepted 27 October 2017
Available online 29 October 2017
0022-2313/ < outputStr5 >

paper presents an alternative strategy towards tuning the PL of Eu doped $SrSO_4$ through post annealing technique. Eu^{2+} and Eu^{3+} co-doped $SrSO_4$ microcrystals were synthesized by employing Eu^{3+} as the sole dopant source in the starting materials. The color of PL from Eu^{2+} and Eu^{3+} co-doped $SrSO_4$ can be tuned from purplish pink through white to bluish purple as the annealing temperature increases from 200 to 1000 °C. The novelty of this work is the realization of tunable emission color of rare-earth doped $SrSO_4$ by simply controlling the post thermal annealing temperature of the sample. Additionally, defect induced emission is observed in $SrSO_4$ at elevated annealing temperature. Mechanisms of the tunable PL are discussed for Eu^{2+} and Eu^{3+} co-doped $SrSO_4$, the roles of V_O in the emissions are addressed.

2. Materials and characterizations

Analytical reagents $Sr(NO_3)_2$, Na_2SO_4 and $Eu(NO_3)_3{\cdot}6H_2O$ were used as the starting materials. In a clean beaker, solution A was prepared by dissolving $Sr(NO_3)_2$ (0.04 mol) and $Eu(NO_3)_3{\cdot}6H_2O$ (0.002 mol) in 100 mL deionized water. In a similar way, solution B was prepared in a separate beaker by dissolving Na_2SO_4 (0.04 mol) in 100 mL deionized water. Under vigorous stirring with a magnetic bar, white precipitates were formed as solution A was slowly dropped into solution B. The white precipitates were filtrated, washed with deionized water, and then dried in an oven at 60 °C for overnight. The dopant concentration of Eu in $SrSO_4$ was 5 mol%.

X-ray diffraction (XRD) spectra were recorded on an X-ray diffractometer (D/max 2500 PC, Rigaku Corporation, Japan) using Cu Kα radiation (λ = 0.15405 nm). The voltage applied to the Cu target in the XRD machine was 40 kV. The scanning electron microscope (SEM) (S-4800, Hitachi, Japan) was employed to analyze the morphology and elemental composition of the phosphor. The accelerating voltage applied to the electron gun in the SEM was 15 kV. The SEM was coupled with a silicon drifted detector as the X-ray analyzer for the energy dispersive X-Ray (EDX) spectroscopic analysis. The PL spectra of the phosphors were recorded with a spectrophotometer (Tianjin Gangdong Ltd., China). The 325-nm laser line from a helium-cadmium laser was utilized as the excitation source for the PL measurement. The PL excitation spectra of phosphors were measured with the fluorescence spectrometer F-7000 (Hitachi, Japan).

First-principles density functional theory (DFT) calculations of the electronic structures of $SrSO_4$ were performed using the DFT module of the Quantumwise Atomistix ToolKit 11.8 package. The exchange-correlation functional was treated within the generalized gradient approximation (GGA) scheme by the Perdew Burke Ernzerhof potential [12]. Orthorhombic $SrSO_4$ belongs to space group *Pnma* (62). There were 4Sr, 4S and 16O atoms in the unit cell of $SrSO_4$. The initial structural data of $SrSO_4$ were taken from Inorganic Crystal Structure Database (ICSD no 85808). The lattice parameters of a = 0.8359 nm, b = 0.5351 nm and c = 0.6869 nm were used in present work. The considered electronic configurations were $3d^{10}4p^65s^2$ for Sr, $2s^22p^4$ for O and $3s^23p^4$ for S. Double zeta single polarized basis sets were chosen for each element. The electronic wave-functions were expanded in plane waves up to a kinetic energy cut-off with a typical value of 100 Hartree. The Monkhorst-Pack scheme k-points grid sampling was set at 5×5×5 for the Brillouin zone. The Brillouin zone sampling and the kinetic energy cutoff were sufficient to guarantee an excellent convergence for the calculated bandstructures.

3. Results and discussions

3.1. Crystal structure and morphology of Eu^{2+} and Eu^{3+} co-doped $SrSO_4$

Fig. 1(a) show the XRD curve of Eu^{2+} and Eu^{3+} co-doped $SrSO_4$ without any subsequent treatment. The diffraction peaks in Fig. 1 are located at 20.984, 23.579, 25.932, 27.039, 28.063, 30.043, 32.765, 33.484, 34.714, 37.817, 39.984, 40.835, 42.173, 44.346, 45.329, 46.610 and 49.013°. According to JCPDS 05-0593, these peaks can be assigned to the reflections from the 011, 111, 002, 210, 102, 211, 112, 020, 301, 212, 220, 103, 221, 113, 401, 410 and 321 crystallographic planes of $SrSO_4$, respectively [6,8,10,13]. Thus Fig. 1(a) has confirmed the formation of orthorhombic $SrSO_4$ via the precipitation route. It is well known that the lattice parameters of the standard $SrSO_4$ are a = 0.8359 nm, b = 0.5352 nm, c = 0.6866 nm, and $\alpha = \beta = \gamma = 90°$. We have noticed the narrow full width at half maximum (FWHM) of each diffraction peak in Fig. 1(a) even before considering the instrumental broadening effect. According to Scherrer equation, the mean value of the crystallite sizes in the sample is larger than 100 nm [14]. Furthermore, we performed the structural refinement using the Rietveld method through wide pattern fitting of the XRD spectrum in Fig. 1(a). For Eu^{2+} and Eu^{3+} co-doped $SrSO_4$, the refined unit cell parameters are a = 0.8365 nm, b = 0.5349 nm and c = 0.6869 nm for the Eu^{2+} and Eu^{3+} co-doped $SrSO_4$. It is obvious that the calculated lattice parameters are very close to those of the standard $SrSO_4$.

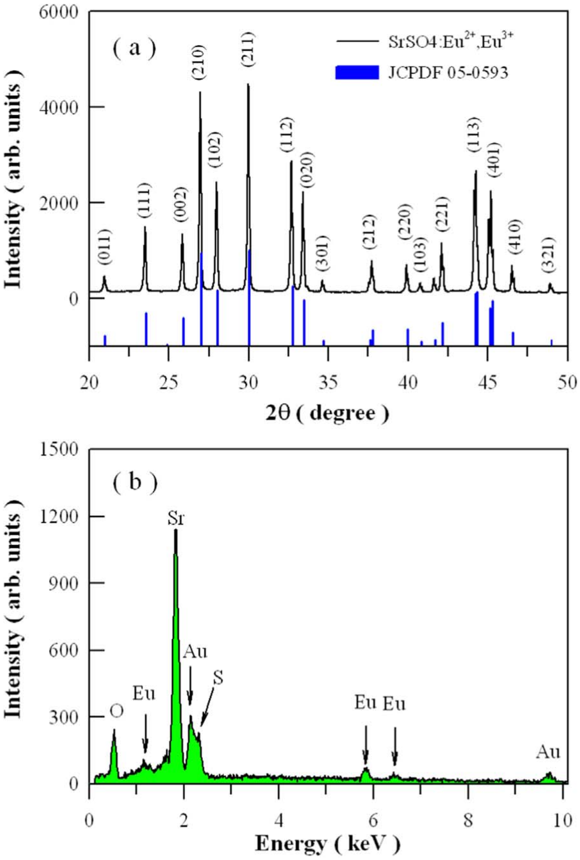

Fig. 1. XRD curve (a) and EDX spectrum (b) of Eu^{2+} and Eu^{3+} co-doped $SrSO_4$ without any subsequent treatment.

EDX is an analytical technique used for the elemental analysis of a specimen. Fig. 1(b) stands for the EDX spectrum of the Eu^{2+} and Eu^{3+} co-doped $SrSO_4$. As can be seen in Fig. 1(b), the three peaks at 0.53, 1.81 and 2.31 keV can be attributed to the characteristic X-ray emissions of O($K\alpha_1$), Sr($L\alpha_{1,2}$) and S($K\alpha_{1,2}$), respectively. Additionally, the X-ray emissions of Au($M\alpha_1$) and Au($L\alpha_1$) are identified at 2.122 and 9.713 keV. The Au element was introduced in the specimen during Au sputtering for the convenience of SEM analysis. These data have confirmed the presence of Sr, O and S in the phosphor. In particular, the characteristic emissions of Eu appear at 1.131 keV (Eu $M\alpha_1$), 5.845 keV (Eu $L\alpha_1$) and 6.456 keV (Eu $L\beta_1$), respectively. The successful detection of Eu rests on the fact that the concentration of Eu in $SrSO_4$ (5 mol%) is higher than the detection limit of the X-ray detector in the EDX instrument (about 3 mol%). Consequently, the results in Fig. 1(b) confirm the chemical composition of Eu doped $SrSO_4$.